IOP PUBLISHING JOURNAL OF PHYSICS D: APPLIED PHYSICS

J. Phys. D: Appl. Phys. **46** (2013) 125201 (9pp) doi:10.1088/0022-3727/46/12/125201

# Control of ion activation energy delivered to tissue and sensitive materials in atmospheric pressure plasmas using thin porous dielectric sheets

**Natalia Yu Babaeva and Mark J Kushner**[1]

University of Michigan, Department of Electrical Engineering and Computer Science 1301 Beal Ave., Ann Arbor, MI 48109-2122, USA

E-mail: nbabaeva@umich.edu and mjkush@umich.edu

Received 17 November 2012, in final form 25 January 2013
Published 18 February 2013
Online at stacks.iop.org/JPhysD/46/125201

**Abstract**

In atmospheric pressure discharges, such as dielectric barrier discharges (DBDs), it is common to have transient sheaths having electric fields of hundreds of kV cm$^{-1}$. With these sheaths, even with short mean free paths, it may be possible to deliver short pulses of energetic ions (tens to hundreds of eV) to surfaces. The energies of these ions can be controlled to some extent by selecting the relative permittivity ($\varepsilon/\varepsilon_0$) of the underlying surface. In using DBDs to treat sensitive materials or tissue in plasma medicine where control of ion energies may be desirable, one has a very limited ability, if any, to modify the dielectric properties of the tissue. In this paper, we use results from a computational study to propose a method to control the characteristics of the transient sheath formed at the surface of sensitive materials or biological tissue by using a thin porous film placed on top of the surface. By controlling the transient sheath, one can control the ion energies delivered to the surface. We show that ion energies delivered to the underlying surface through the pores can be controlled by the capacitance and thickness of the film and the width of the pore. Results are discussed for streamer penetration and ion energies delivered to the surface when the plasma filament directly strikes the pore and is offset from the pore.

(Some figures may appear in colour only in the online journal)

## 1. Introduction

Plasmas generated in atmospheric pressure dielectric barrier discharges (DBDs) are frequently used to functionalize the surfaces of polymers and are now being investigated for treatment of living tissue in the context of plasma medicine [1–10]. Surfaces in contact with DBDs are simultaneously exposed to chemically reactive neutral radicals produced by the discharge, UV radiation and ion bombardment. Recently, there have been extensive studies on production of radicals from atmospheric pressure plasmas as might be used in plasma medicine applications [5, 11, 12]. However, the role of kinetically energetic particles, such as ions produced by the plasma, is less thoroughly investigated. Ions having energies of many keV are capable of sputtering cell membranes and biological tissue, though these energies are well beyond those expected in DBDs [9]. It has been proposed that the therapeutic effects of cold atmospheric plasmas in direct contact with living tissue may be partly attributed to less energetic ions impinging onto wounds and tissue surfaces [8]. Although these ions probably do not penetrate beyond the top layers of cells, their energetic fluxes are non-negligible.

In our previous work [13], we found that nanosecond pulses of ions with energies in excess of tens of electron volts (eV) can be delivered to the surfaces of dielectrics by DBDs. Although the mean free path of ions at atmospheric pressure is $<1\,\mu$m, the formation of transient sheaths at the

[1] Author to whom any correspondence should be addressed.

 

dielectric surface with electric fields of hundreds of kV cm$^{-1}$ is capable of delivering these energetic ions. Little is known about the consequences of ions of tens to a hundred eV incident onto biological surfaces, however recent molecular-dynamics simulations of lipid-like materials resembling cell members indicate that these ions are not benign [14] and may produce significant sputtering of carbon atoms. These results motivate one to devise the means to control these ion energies.

In this regard, we found that ion energies delivered onto dielectric surfaces can be controlled to some extent by layering the dielectric substrate [13]. In this manner the applied voltage is divided between the resistance of the plasma column, the sheath at the dielectric surface, and the layered capacitances of the substrate. By varying the dielectric constant of the material underlying the top surface to be treated, as might be possible in the treatment of thin polymer sheets, the energies of ions incident onto the top surface can be controlled. If the surface being treated is bulk material, for example human tissue, one unfortunately has a very limited ability, if any ability at all, to change the dielectric properties under the surface to be treated to in order to control the ion energies delivered to the top surface.

In this paper, we use results from a computational investigation to propose a method to control the transient sheath formed at the surface of sensitive bulk materials and biological tissue by atmospheric pressure plasmas such as DBDs. By controlling the transient sheath, one can control the ion energies delivered to the surface. In this method, a thin dielectric film is placed on the surface. The film has small holes through which the plasma streamers can partially penetrate. We show that ion energies can be controlled by the capacitance and thickness of the film and the size of the hole. A film having a large permittivity expels the electric field. If the size of the pores in the film are smaller or commensurate with the width of the filament, the sheath is moulded over the surface of the pore and the potential expelled from the dielectric is partly retained in sheath, thereby increasing the electric field in the sheath. By varying the permittivity of the dielectric sheet, this electric field can be controlled and so the ion energies incident onto the underlying surface through the pores can be controlled as well.

The model used in this investigation is briefly described in section 2. We discuss ion energy and angular distributions (IEADs) delivered to the underlying surface covered by a thin porous dielectric film for plasma filaments arriving directly over the pore in section 3. A discussion of IEADs for filaments not directly over the pore is in section 4. Our concluding remarks are in section 5.

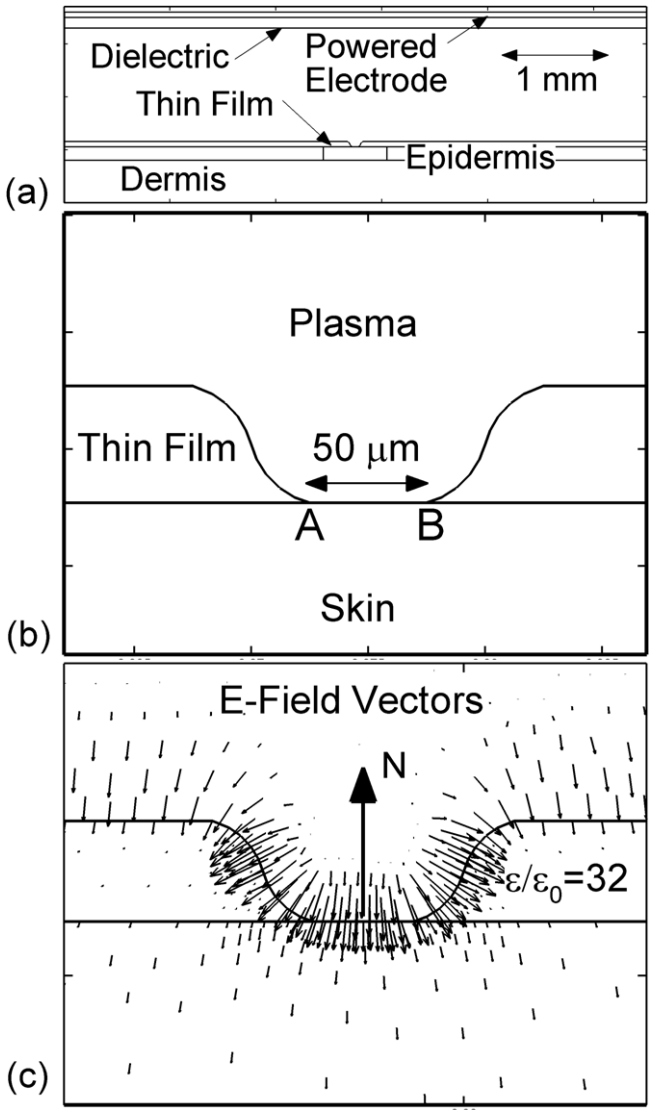


**Figure 1.** Geometry used for simulation of a single DBD filament and IEADs incident onto a porous thin film covering the skin to be treated. (*a*) Total computational domain. The top powered electrode is covered by dielectric ($\varepsilon/\varepsilon_0 = 3$) with thickness of 80 $\mu$m. The bottom grounded electrode is covered with 400 $\mu$m tissue representing dermis ($\varepsilon/\varepsilon_0 = 3$) and 100 $\mu$m tissue representing epidermis ($\varepsilon/\varepsilon_0 = 4$). In addition, the tissue being treated is covered by thin porous dielectric with variable dielectric constant. (*b*) Close-up of the pore. The area AB indicates the surface where the ions are collected. (*c*) Typical electric field vectors for an approaching plasma filament and the normal vector $\boldsymbol{N}$ defining zero-angle for incident ions.

## 2. Description of the model

IEADs delivered by plasma filaments to underlying materials in DBDs intersecting with a thin porous dielectric film was computationally investigated using the modelling platform, *nonPDPSIM*. This model is the same as used in [13–15], and so will be only briefly discussed here. *nonPDPSIM* is a two-dimensional simulation implemented on an unstructured numerical mesh in which Poisson's equation and transport equations for charged and neutral species are solved. Poisson's equation is solved throughout the entire computational domain (except in metals where the potential is specified as a boundary condition). Continuity equations for gas phase charged and neutral particles are only solved outside solid materials while conservation equations for surface and volume charge are solved on and inside all non-metallic materials. The unstructured mesh consisted of approximately 8100 nodes, of which about 6000 are in gas phase regions where plasma may exist. The plasma is sustained in 1 atm of dry air having $N_2/O_2 = 80/20$. The species included in the model and the reaction mechanism are similar to those discussed in [14].

IEADs to surfaces are computed using the plasma chemistry Monte Carlo module (PCMCM), as described in [13]. The mesh spacing for the PCMCM used to model the kinetic transport of ions into the surface was 0.25–0.5 $\mu$m.

A schematic of the model geometry for DBD treatment of, for example, skin through a porous dielectric film is shown in figure 1. The entire computational domain is 5.5 mm × 2 mm. The materials underlying the film are dielectrics having the electrical properties approximating that of human skin. (The epidermis and dermis are not resolved at the cellular level). The dermis has relative permittivity $\varepsilon/\varepsilon_0 = 3$ and the epidermis, 127 $\mu$m thick, has relative permittivity $\varepsilon/\varepsilon_0 = 4$.

The upper powered electrode is covered with a 80 $\mu$m thick dielectric separated by 1 mm from the thin film. The upper electrode at the top of the computational domain was powered while the boundary of the bottom of the computational domain was grounded thus imposing Dirichlet boundary conditions. The left and right boundaries used von Neumann boundary conditions. The positive filaments are initiated by a small cloud of seed electrons and $N_2^+$ placed near the upper dielectric having a peak density of $10^9$ cm$^{-3}$ and a Gaussian profile (50 $\mu$m in the horizontal direction and 100 $\mu$m in the vertical direction). The filament is then naturally sustained by its own space charge driven electric field and by secondary emission from surfaces. The opposite dielectric is initially uncharged and the DBD voltage is +15 kV. The filaments are launched directly over a pore in the thin film or shifted a few hundred micrometres to the left of the pore. The porous thin film has thickness of 50 $\mu$m. The width of the pore is 100–150 $\mu$m, at the top with the exposed skin being 25–50 $\mu$m at the bottom. The porous film has a dielectric constant of 2, 8, 16, 32 or 80. IEADs are averaged over the exposed skin between points A and B (shown in figure 1(*b*)) with respect to the normal perpendicular to the skin surface. Ions arriving to the right of the normal have positive angles, while ions arriving to the left have negative angles. Throughout this paper, the surface treated, the *exposed surface*, is the surface of the underlying polymer (or skin) which is exposed by the opening in the pore. This is the surface line between A and B shown in figure 1(*b*).

## 3. IEADs through a pore to underlying skin

The shape of the sheath, the distribution of electric field within the sheath and the mean free path for ions traversing the sheath generally determines the characteristics of IEADs arriving onto the surface. In this case, the shape of the sheath can be influenced by the pore topology, the dielectric constant and conductivity of the thin film and the epidermis and dermis layers underneath the dielectric film. If the size of the sheath is commensurate to the size of the pore, the sheath may conformally adhere to the contour of the pore (often referred to a plasma moulding) which then modifies the orientation of the electric field and ion trajectories [16]. This is particularly the case in low-pressure plasmas where plasma moulding around and into corners generally determines the shape of IEADs to the underlying materials [17, 18].

In the heads of filaments in DBDs, an ionization wave, electric fields can exceed 200 kV cm$^{-1}$ when the filament is far from a surface. When the filament strikes the surface, the voltage across the head of the filament is transferred to sheath that forms at the surface and if the underlying material is a dielectric, into that material. The degree of electric field compression depends on the dielectric constant $\varepsilon/\varepsilon_0$ of the surface. Upon intersection of the filament with the surface, the electric fields in the sheath can exceed 400–800 kV cm$^{-1}$. Since materials having larger $\varepsilon/\varepsilon_0$ tend to exclude electric field lines, the electric field in the sheath captures more of the transferred voltage and so the field in the sheath is larger when intersecting materials with larger $\varepsilon/\varepsilon_0$. When accelerated in these fields, ions can gain energies across their mean free path (0.5–1 $\mu$m) up to tens of eV for dielectrics striking materials with low $\varepsilon/\varepsilon_0$ and up to a hundred eV for striking dielectrics with high $\varepsilon/\varepsilon_0$ [13].

Positive plasma filaments are launched from the upper dielectric directly over a pore with an exposed width of 50 $\mu$m. The powered electrode voltage is 15 kV. The evolution of electron density and electron impact ionization sources, $S_e$, are shown in figure 2 on streamer and pore spatial scales. The enlargement in the pore also shows electric field vectors and electric potential contours. Typical maximum plasma densities are $5 \times 10^{14}$ cm$^{-3}$. When the plasma strikes the surface of the film, the plasma spreads over the surface as a surface resident ionization wave and penetrates into the pore. The surface streamer spreads to a width of 3 to 5 mm in about 3.3 ns. In a multi-filament DBD, the intersection of adjacent surface streamers likely prevents excessive spreading of plasma on the dielectric resulting in self-organized plasma spots [19, 20]. Since the size of the pore is commensurate to the width of the streamer and much larger than the Debye length, the streamer is able to penetrate into the pore. In doing so, a sheath is conformally produced along the boundary of the pore, compressing potential contours, and reorienting the direction of the electric field to be nearly perpendicular to the surface (as also shown in figure 1(*c*)).

The electron impact ionization sources, shown in figure 2(*b*), are indications of the location of the avalanche front in the bulk and surface streamers. This intense electron impact ionization, up to $9 \times 10^{25}$ cm$^{-3}$ s$^{-1}$, takes place in the head of the streamer when the filament is far from the surface. As the streamer intersects the surface, charging of the surface produces electric field components parallel to the surface, which then spreads the plasma towards uncharged surfaces. This is accompanied by an ionization wave along the surface with speeds up to $1.4 \times 10^8$ cm s$^{-1}$. The ionization sources also penetrate into the pore, first in the volume of the pore and then dominantly in the sheath. This ionization source close to and in the sheath provides a local source of ions that can be accelerated by the sheath into the exposed surface of the underlying skin.

When the filament strikes a flat surface, the majority of the applied voltage is momentarily transferred to the sheath formed at the surface. This results in electric fields in the sheath being many hundreds of kV cm$^{-1}$ lasting for a few ns. The voltage dropped across the sheath is in part determined by voltage division between the underlying surface and the sheath. If the surface is multi-layered (as is the case here when

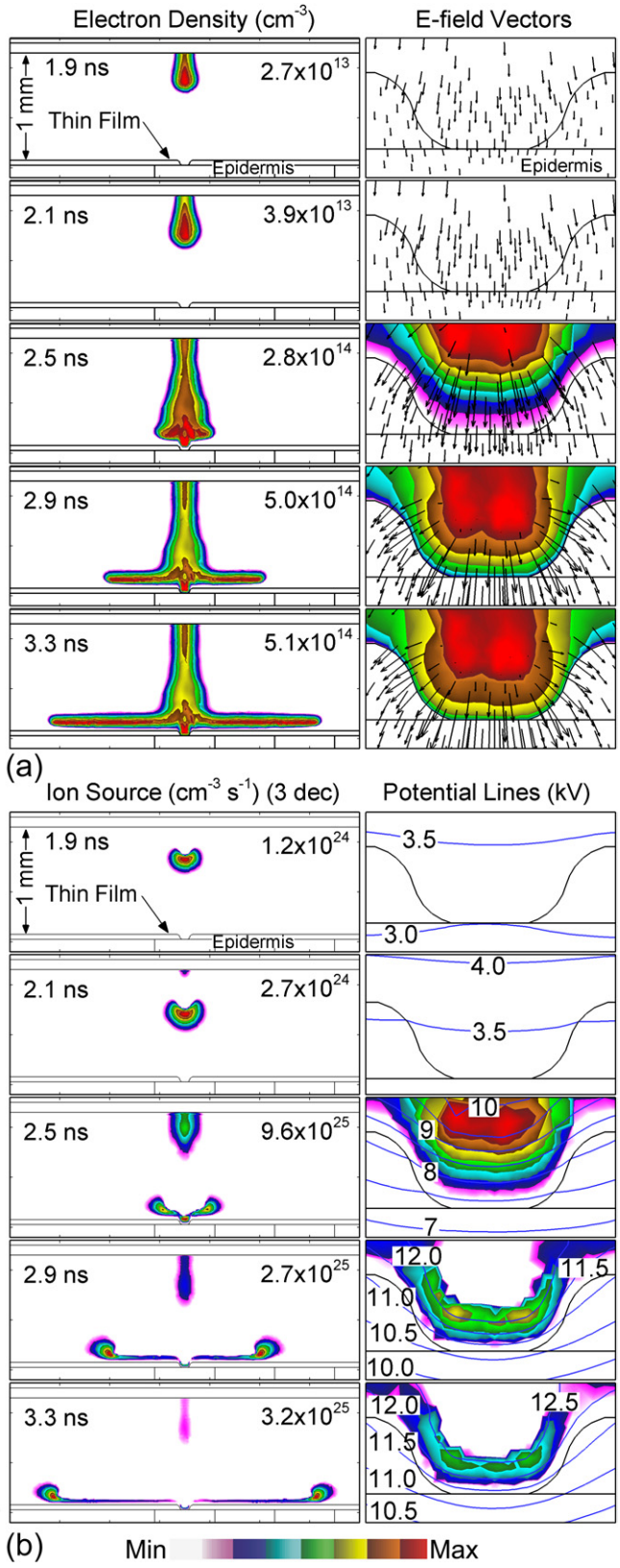


**Figure 2.** Time sequence of (*a*) electron density and electric field vectors and (*b*) electron impact source and potential lines for a positive filament arriving directly over a pore in the thin film ($\varepsilon/\varepsilon_0 = 2$). As the plasma filament (conditions: dry air, +15 kV) approaches the pore, the plasma penetrates the pore and spreads over the dielectric. The contours are plotted on a log scale over three decades with the maximum value shown in each frame. All the frames have the same horizontal and vertical scale.

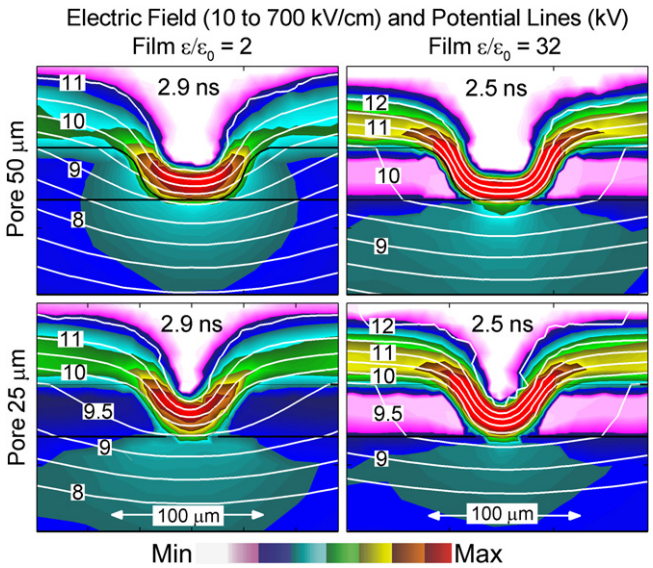


**Figure 3.** Electric field (flood) and potential (lines) at the moment when the plasma filament approaches the surface and steady-state sheath is formed over the pore. Results are shown for films having (left) $\varepsilon/\varepsilon_0 = 2$ and (right) $\varepsilon/\varepsilon_0 = 32$; and for pore dimension of (top) 50 $\mu$m and (bottom) 25 $\mu$m. The sheath is typically thicker for larger $\varepsilon/\varepsilon_0$ and smaller pore dimension. All the frames have the same horizontal and vertical scale.

a film is placed on top the skin), the voltage division will be between the stack of capacitance. Less voltage is dropped across surface films having larger capacitance, that is larger values of relative permittivity $\varepsilon/\varepsilon_0$, and so a larger proportional voltage is dropped across the sheath. If one of the materials is resistive, additional voltage is dissipated across that resistance.

When the filament intersects a surface having a pore that is commensurate to the thickness of the sheath, the sheath will conformally line the pore. For example, the moulding of the sheath over 50 and 25 $\mu$m pores in films having $\varepsilon/\varepsilon_0 = 2$ and 32 is shown in figure 3 where the magnitude of the electric field and electric potential contours are plotted. The potential contours that are expelled from the film and are contained in the sheath on the top flat surface tend to follow the sheath into the pore. This results in an electric field in the sheath on the surface of the exposed skin being similar, and in some cases larger, than that on top of the film. The higher the dielectric constant of the thin film, the more potential lines are expelled from the interior of the film and are captured in the sheath within the pore. The potential drop across the sheath lining the 50 $\mu$m pore is 1 kV for a film with $\varepsilon/\varepsilon_0 = 2$ and 2 kV for a film with $\varepsilon/\varepsilon_0 = 32$.

The voltage drops across the sheath are functions of the pore size. The sheaths lining smaller pores retain more of the expelled potential and so produce larger electric fields. For example, the potential drop across the sheath lining the 25 $\mu$m pore is almost 2 kV for the film with $\varepsilon/\varepsilon_0 = 2$ and 2.5 kV for the film with $\varepsilon/\varepsilon_0 = 32$. (See figure 3.) The properties of the sheath are mostly determined by the material properties of the porous film rather than the properties of the underlying tissue being treated. Note, that the width of the pores should not greatly exceed the thickness of the sheaths. In cases where the width of the pore is much larger than the width of the sheaths,

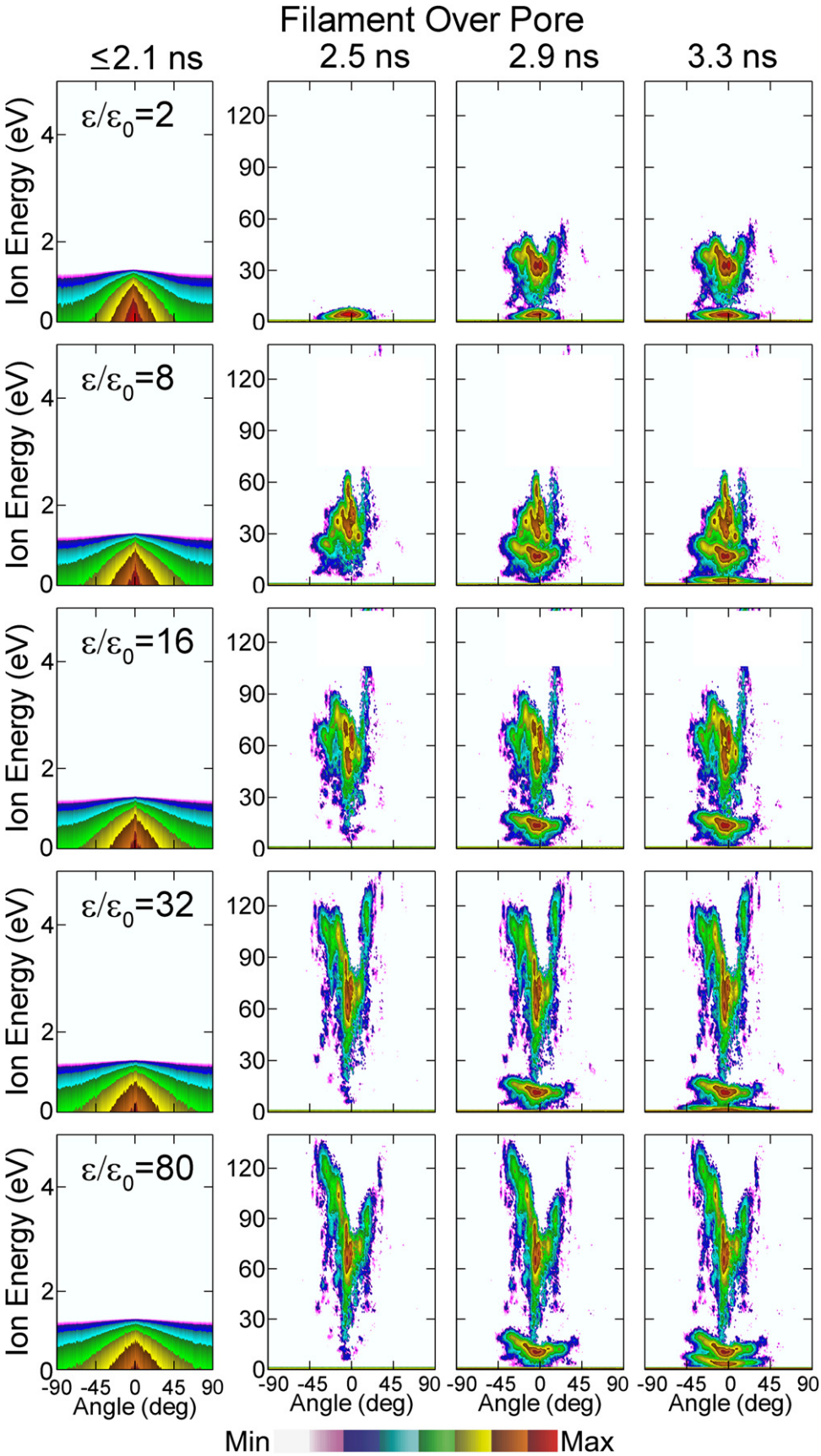


**Figure 4.** IEAD as a function of time and $\varepsilon/\varepsilon_0$ of the porous dielectric for a plasma filament arriving directly over pore. The times correspond to the filament positions shown in figure 2. When the filament is far from the pore, ions arrive at the surface essentially thermalized (<2.1 ns). When filaments strike the surface and a transient sheath is formed, IEADs have a V-shape reflecting the divergence of electric field inside the pore. The contours are plotted on a log scale over four decades.

the properties of the sheath on the skin are largely determined by the properties of the tissue itself and not the film.

With potential drops of 2–3 kV in the sheath, the sheath thickness is a few tens of $\mu$m. This results in electric fields of the order of a few hundreds of kV cm$^{-1}$ lasting for many ns. With mean free paths below 1 $\mu$m for ions at atmospheric pressure, one might expect ion energies of up to tens of eV incident onto the exposed surface produced by acceleration in the sheath. The time evolution of IEADs for $O_2^+$ incident onto the exposed surface of a 50 $\mu$m pore for films with various dielectric constants is shown in figure 4. (IEADs are averaged between A and B indicated in figure 1(*b*).) The times for which the IEADs are recorded correspond to the time frames shown in figure 2. Prior to the filament arriving at the surface of the film ($t < 2.5$ ns), a small flux of ions to the surface is produced by photoionization ahead of the filament. These ions drift in the local electric field at the surface, <60 kV cm$^{-1}$, unperturbed by net charge density and arrive on the surface with energies not exceeding 1 eV. These energies are essentially the same as given by the effective temperature of ions drifting in an electric field ($3/2k_B T_{eff} = 3/2k_B T_I + 1/2Mv_D^2$, $T_I$ = ion temperature, $T_{eff}$ = effective ion temperature, $v_D$ = drift velocity) [21]. The IEADs have a V-shape for high permittivities of the film, a consequence of ions striking near the edge of the pore where the electric field is oriented at an angle from the vertical. (See figure 1(*c*).)

When a filament strikes the exposed surface at the bottom of the pore, the ion energies striking that surface increase up to 40 eV for the film having $\varepsilon/\varepsilon_0 = 2$. The maximum ion energy increases with increasing dielectric constant of the film up to $\varepsilon/\varepsilon_0 > 16$ for which ion energies exceed 100 eV, as shown in figure 5. Maximum ion energies as a function of pore width and $\varepsilon/\varepsilon_0$ of the film are shown in figure 6. For $\varepsilon/\varepsilon_0 > 16$ ion energies do not appreciably increase, a consequence of the majority of the potential lines having already been expelled from the film. The sheath is sufficiently thick (20–30 $\mu$m) that ions cannot collisionlessly traverse the sheath, and so arrive at the surface with energies significantly below the sheath potential of a few kV. The sheath is collisional for electrons as well and so ionizing collisions occur within the sheath. The IEADs have a low energy component resulting from ions formed close to the surface or having their last collision in close vicinity of the surface (hundreds of nm). The IEADs also have a high energy component resulting from ions having had a free flight of their full mean free path (about 0.5 $\mu$m). The surface at the bottom of smaller pores with the same dielectric constant receive more energetic ions, as shown in figures 5 and 6. Less moulding of the sheath into the smaller pore results in more electric potential lines being retained in the sheath.

When averaged over the exposed surface at the bottom of the pore, the IEADs have V-shapes with the highest energy for ions being incident at non-normal angels. This results from the finite thickness of the sheath attempting to mould over the curvature of the pore, which then produces curvature in the equipotential lines above the exposed surfaces, as shown in figure 3. The resulting electric field vectors intersect the surface at non-normal angles. (See figures 1(*c*) and 2.)

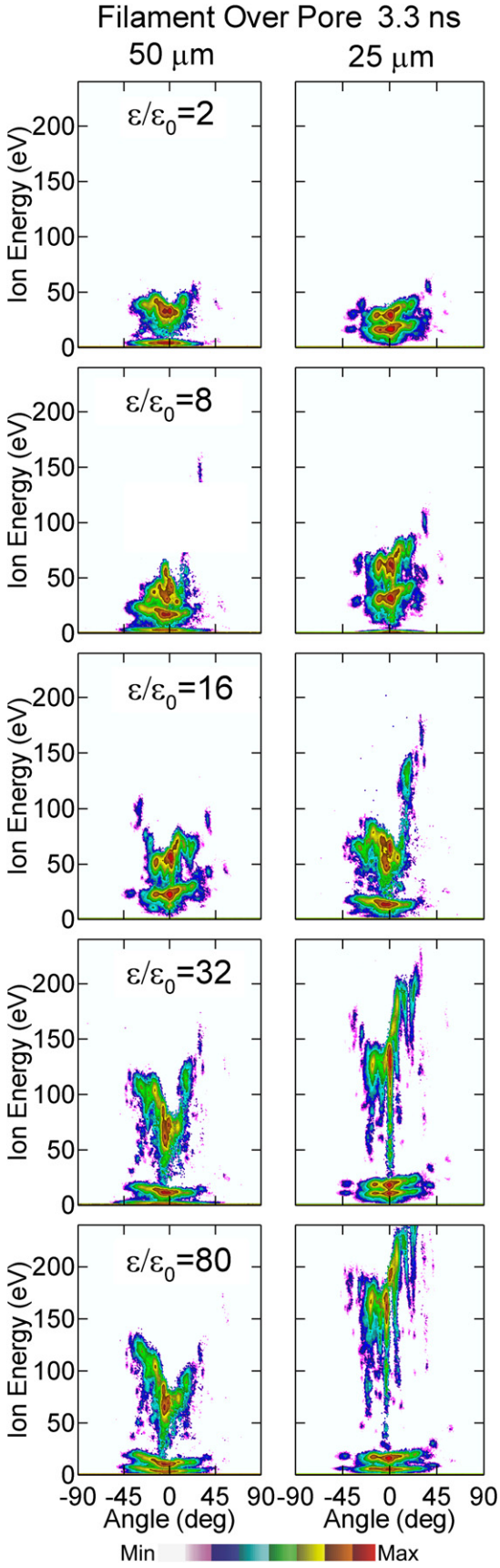


**Figure 5.** IEADs for dielectric constant of the porous film of 2 to 80 for a pore of width (left) 50 $\mu$m and (right) 25 $\mu$m. The ion energies increase with increasing $\varepsilon/\varepsilon_0$. For the same dielectric constant, ion energies are higher for the smaller pore due to there being less moulding of the sheath over the pore.

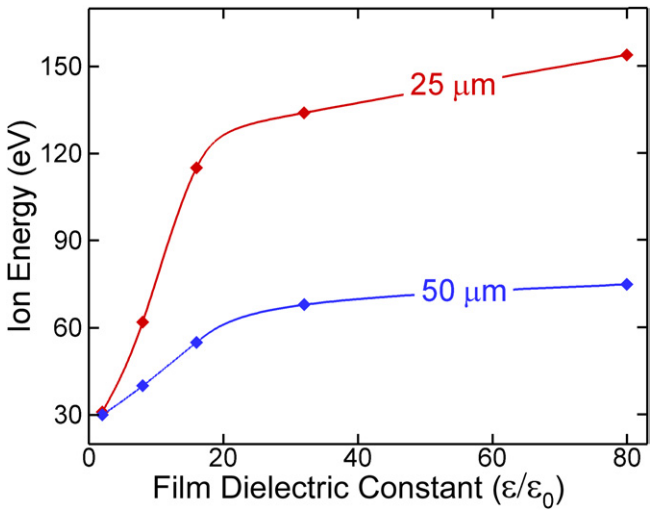


**Figure 6.** Maximum ion energy incident on the exposed surface (the line AB indicated in figure 1(*b*)) as a function of dielectric constant for the film for 25 and 50 $\mu$m pores .

## 4. IEADs from filaments shifted from the pore

It is likely that plasma filaments will strike the film at locations shifted from the axis of the pore. IEADs were therefore investigated for filaments striking 300 and 600 $\mu$m from the centre of the pore. The evolution of electron density and ion sources for the filaments striking 300 $\mu$m to the left of the 50 $\mu$m pore is shown in figure 7. The overall behaviour of the filament (as indicated by [e] and $S_e$) is nearly indistinguishable from the case where the filament is directly over the pore. As the plasma spreads along the surface with a sheath thickness of about 30 $\mu$m, the surface filament enters into the pore. The enlarged images of the pore in figure 7 show the plasma entering into the pore from the left side. The electric potential and electric field vectors are skewed towards the right inner surface of the pore, which preferentially produces ionization on the right side. This asymmetry results from the horizontal components of the electric field at the head of the surface discharge as it spreads on the surface. As the filament fills the pore and the surface discharge is on both sides of the pore, much of this asymmetry dissipates.

IEADs produced by filaments shifted from the pore by 300 and 600 $\mu$m for thin films with $\varepsilon/\varepsilon_0 = 2$ and 32 are shown in figure 8. Before the plasma covers the pore ($t < 2.5$ ns) ions arrive on the treated surface at grazing angles. After the plasma covers the pore and a steady state sheath is formed (albeit for only a few ns), the IEADs are almost symmetric at high energies. However, for lower and thermal ion energies, the IEADs are shifted to positive grazing angles. This asymmetric IEAD results from the lateral components of the electric field which spreads the plasma on the surface.

Additional simulations (not shown here) with pores shifted by 900 $\mu$m were also conducted. We found that there is no significant decrease in the energy of ions delivered into pores for filaments shifted by as much as 900 $\mu$m from the pore. As long as the voltage drop along the surface of the film as the filament spreads is small compared to applied voltage, the lateral electric field producing the spreading ionization wave

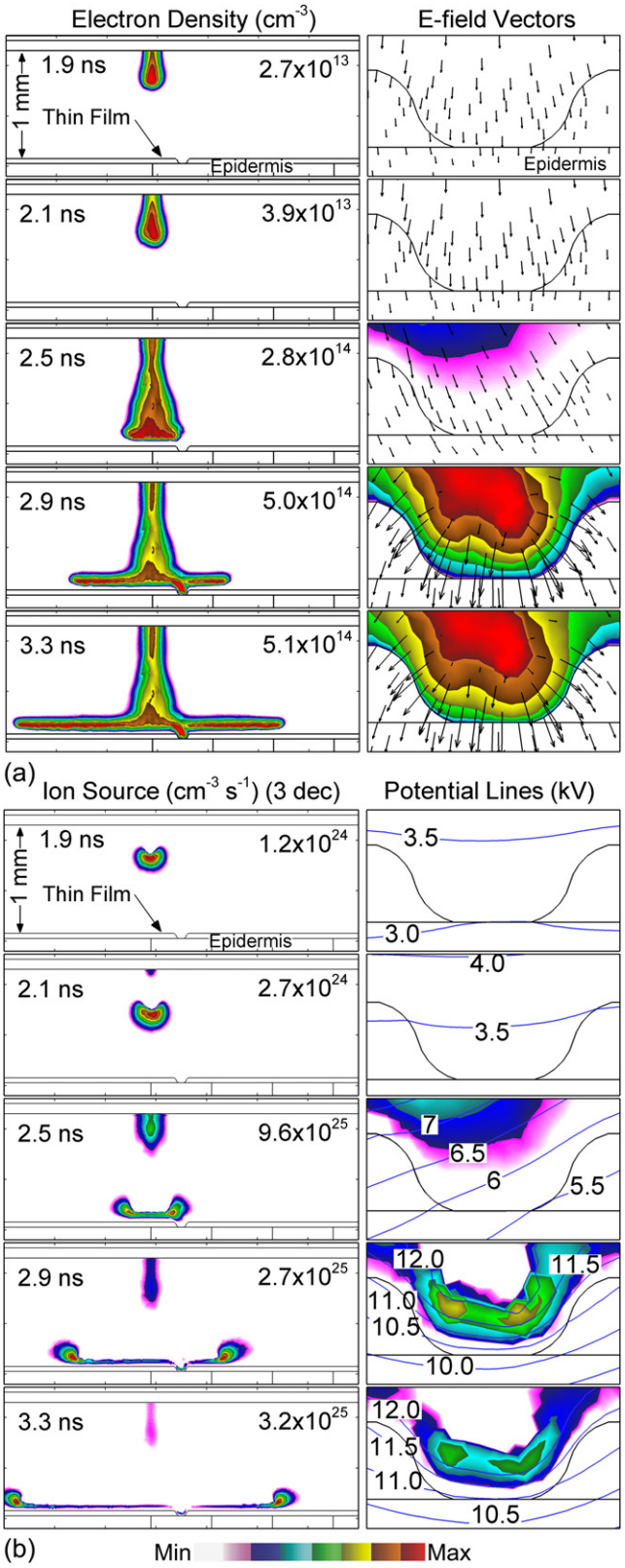


**Figure 7.** Time sequence of (*a*) electron density and electric field vectors and (*b*) electron impact source and potential lines for a positive filament arriving 300 $\mu$m to the left of the pore. The contours are plotted on a log scale over three decades with the maximum value shown in each frame. All the frames have the same horizontal and vertical scale.

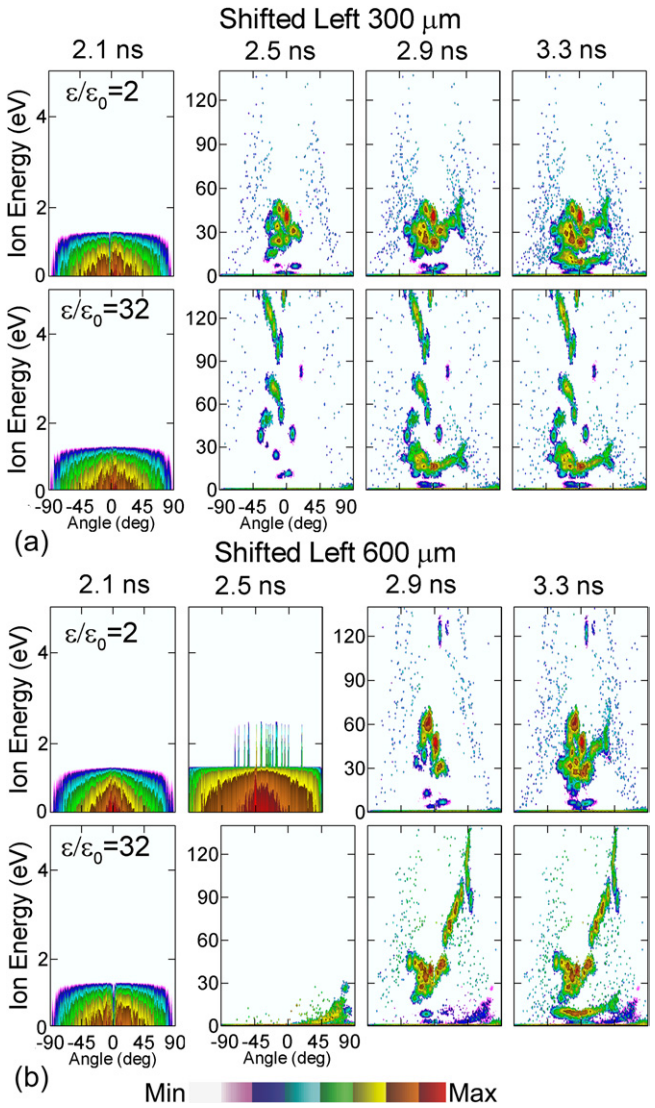


**Figure 8.** IEADs as a function of time for a plasma filament shifted (*a*) 300 $\mu$m and (*b*) 600 $\mu$m to the left of the pore. The times correspond to the filament positions shown in figure 7. The contours are plotted on a log scale over four decades.

will not significantly change. As a result, the sheath forming in the pore will not significantly change. The filaments in DBDs operating at a few tens of kV have separations no greater than 500 $\mu$m to 1 mm. As such, we might expect that the exposed bottom of the pore will be uniformly treated. In actual treatment of a surface, the film may have many pores to treat a large area. As a result the spreading filament will move into and out of many mores. We conducted simulations where the filament spread into and out of two pores separated by 600 $\mu$m, and found no significant difference in the IEADs delivered into the pore.

## 5. Concluding remarks

Even with a mean free path of less than a micron, ion energies delivered to surfaces by the large electric fields of DBD filaments can exceed many tens of eV. In the context of surface treatment, and plasma medicine in particular, it may be desirable to control these ion energies. We proposed a method of controlling IEADs to the surface by use of a porous dielectric thin film. By changing the dielectric constant and width of the pores, one can control the energies of ions incident onto the underlying surface. The maximum energies delivered to the exposed surface generally increase with increasing $\varepsilon/\varepsilon_0$ of the film and decreasing width of the pore. These trends apply for conditions where the plasma filament strikes the pore and when the spreading surface discharge flows into the pore. Since the pores will expose only a fraction of the underlying surface even with a film having many pores, uniform treatment will require that the porous film be translated during treatment. The total fluence to any given surface site will then be smaller compared to uncontrolled treatment. However, the advantageous tradeoff is that one is able to control the ion energies. The simulations reported here addressed conditions correlating to dry skin having a finite conductivity. It is true that treating wounds may involve wet surfaces having higher conductivity. We do not expect the trends reported here to depend critically on the wetness or dryness of the underlying material, as control of the IEADs depend on voltage division between the film and the plasma sheath.

## Acknowledgments

This work was supported by the US Department of Energy Office of Fusion Energy Science and the National Science Foundation.

## References

[1] Strobel M, Lyons C S and Mittal K L (ed) 1994 *Plasma Surface Modification of Polymers* (Zeist, The Netherlands: VSP Press)

[2] Lopez-Santos C, Yubero F, Cotrino J, Barranco A and Gonzalez-Elipe A R 2008 Plasmas and atom beam activation of the surface of polymers *J. Phys. D: Appl. Phys.* **41** 225209

[3] Fang Z, Xie X, Li J, Yang H, Qiu Y and Kuffel E 2009 Comparison of surface modification of polypropylene film by filamentary DBD at atmospheric pressure and homogeneous DBD at medium pressure in air *J. Phys. D: Appl. Phys.* **42** 085204

[4] Papageorghiou L, Panousis E, Loiseau J F, Spyrou N and Held B 2009 Two-dimensional modeling of a nitrogen dielectric barrier discharge (DBD) at atmospheric pressure: filament dynamics with the dielectric barrier on the cathode *J. Phys. D: Appl. Phys.* **42** 105201

[5] Graves D B 2012 The emerging role of reactive oxygen and nitrogen species in redox biology and some implications for plasma applications to medicine and biology *J. Phys. D: Appl. Phys.* **45** 263001

[6] Shekhte A B, Serezhenkov V A, Rudenko T G, Pekshev A V and Vanin A F 2005 Beneficial effect of gaseous nitric oxide on the healing of skin wounds *Nitric Oxide-Biol. Chem.* **12** 210

[7] Fridman G, Shekhter A B, Vasilets V N, Friedman G, Gutsol A and Fridman A 2008 Applied plasma medicine *Plasma Process. Polym.* **5** 503

[8] Kong M G, Kroesen G, Morfill G, Nosenko T, Shimizu T, van Dijk J and Zimmermann J L 2009 Plasma medicine: an introductory review *New J. Phys.* **11** 115012

[9] Morfill G E, Kong M G and Zimmermann J L 2009 Focus on plasma medicine *New J. Phys.* **11** 115011
[10] Laroussi M, Mendis D A and Rosenberg M 2003 Plasma interaction with microbes *New J. Phys.* **5** 41
[11] Sakiyama Y, Graves D B, Chang H-W, Shimizu T and Morfill G E 2012 Plasma chemistry model of surface micro-discharge in humid air and dynamics of reactive neutral species *J. Phys. D: Appl. Phys.* **45** 425201
[12] Murakami T, Niemi K, Gans T, Connell D O and Graham W G 2013 Chemical kinetics and reactive species in atmospheric pressure helium–oxygen plasmas with humid air impurities *Plasma Sources Sci. Technol.* **22** 015003
[13] Babaeva N Yu and Kushner M J 2011 Ion energy and angular distributions onto polymer surfaces delivered by dielectric barrier discharge filaments in air: I. Flat surfaces *Plasma Sources Sci. Technol.* **20** 035017
[14] Babaeva N Yu, Ning N, Graves D B and Kushner M J 2012 Ion activation energy delivered to wounds by atmospheric pressure dielectric-barrier discharges: sputtering of lipid-like surfaces *J. Phys. D: Appl. Phys.* **45** 115203
[15] Xiong Z, Robert E, Sarron V, Pouvesle J-M and Kushner M J 2012 Dynamics of ionization wave splitting and merging of atmospheric-pressure plasmas in branched dielectric tubes and channels *J. Phys. D: Appl. Phys.* **45** 275201
[16] Czarnetzki U, Hebner G A, Luggenholscher D, Dobele H F and Riley M E 1999 Plasma sheath electric field strengths above a grooved electrode in a parallel-plate radio-frequency discharge *IEEE Trans. Plasma Sci.* **27** 70
[17] Kim D and Economou D J 2002 Plasma molding over surface topography: simulation of ion flow and energy and angular distributions over steps in rf high density plasmas *IEEE Trans. Plasma Sci.* **30** 2048
[18] Kim D, Economou D J, Woodworth J R, Miller P A, Shul R J, Aragon B P, Hamilton T W and Willison C G 2003 Plasma molding over surface topography: simulation and measurement of ion fluxes, energies and angular distributions over trenches in RF high density plasmas *IEEE Trans. Plasma Sci.* **31** 691
[19] Stollenwerk L 2009 Interaction of current filaments in dielectric barrier discharges with relation to surface charge distributions *New J. Phys.* **11** 103034
[20] Celestin S, Canes-Boussard G, Guaitella O, Bourdon A and Rousseau A 2008 Influence of the charge deposition on the spatio-temporal self-organization of streamers in a DBD *J. Phys. D: Appl. Phys.* **41** 205214
[21] Mason E A and McDaniel E W 1988 *Transport Properties of Ions in Gases* (New York: Wiley)